Published in final edited form as:
Adv Drug Deliv Rev. 2008 September ; 60(12): 1371–1382. doi:10.1016/j.addr.2008.04.009.

Realizing the potential of the Actinium-225 radionuclide generator in targeted alpha-particle therapy applications

Matthias Miederer[1], **David A. Scheinberg**[2], and **Michael R. McDevitt**[2,*]

[1]Klinik und Poliklinik für Nuklearmedizin, Klinikum rechts der Isar, Ismaningerstr. 22, 81675 München, Germany

[2]Memorial Sloan-Kettering Cancer Center, 1275 York Avenue, Box 231, New York, New York 10021, United States of America

Abstract

Alpha particle-emitting isotopes have been proposed as novel cytotoxic agents for augmenting targeted therapy. Properties of alpha particle radiation such as their limited range in tissue of a few cell diameters and their high linear energy transfer leading to dense radiation damage along each alpha track are promising in the treatment of cancer, especially when single cells or clusters of tumor cells are targeted. Actinium-225 (^{225}Ac) is an alpha particle-emitting radionuclide that generates 4 net alpha particle isotopes in a short decay chain to stable ^{209}Bi, and as such can be described as an alpha particle nanogenerator. This article reviews the literature pertaining to the research, development, and utilization of targeted ^{225}Ac to potently and specifically affect cancer.

Keywords

Actinium-225; ^{225}Ac; alpha particle-emitter; nano-device; targeted therapy; monoclonal antibody; DOTA; radioimmunotherapy

1 Introduction

Targeted therapy for the treatment of malignant diseases is a rapidly growing field and has already achieved critical success with the introduction of FDA approved drugs adding new modalities to the current cancer therapy arsenal of surgery, chemotherapy and external beam radiation. The specificity which is imparted by the targeting vehicle (e.g., antibodies, peptides, tetramers, small molecules) can be complemented by attaching a cytotoxic payload to elicit a very potent therapeutic effect. Particle-emitting radioactive isotopes are some of the most promising cytotoxic moieties when linked to tumor-targeting carrier molecules. To date, much of the work has been done with beta particle-emitting isotopes. Iodine-131 Tositumomab (Bexxar) and Yttrium–90 Ibritumomab Tiuxetan (^{90}Y-Zevalin) are FDA approved beta particle-emitting IgGs used to treat B-cell non-Hodgkin's lymphoma [1].

The increased availability and improved radiochemistry of alpha particle-emitting nuclides for targeted therapy have presented new possibilities for their use in radioimmunotherapy.

*Corresponding author: Tel.: 646-888-2192. m-mcdevitt@ski.mskcc.org.

Alpha particles offer key advantages over beta particles, in particular are the high linear energy transfer (LET) and the limited range in tissue. The high alpha particle LET of approximately 100 keV/μm can produce substantially more lethal double strand DNA breaks per radiation track than beta particles when transversing a cell nucleus. The alpha particle tracks are relatively short and thus have a limited range in tissue (on the order of a few cell diameters). This confines the toxic effect to a relatively small field within a few cell diameters from the site of isotope decay versus the much longer-ranged beta particles. ^{90}Y for example, has a maximum range on the order of several hundred cell diameters and thus deposits energy in the tumor as well as the surrounding normal tissue. The number of particle track transversals through a tumor cell nucleus that is necessary to kill the cell is considerably lower for alpha particles than for beta particles and it has been estimated that one alpha particle transversal can kill a cell [2]. This higher biological effectiveness seems nearly independent of oxygen concentration, dose rate and cell cycle position.

Preclinical research has demonstrated the potential of alpha particle-emitting isotopes in radioimmunotherapy (reviewed in [3]). Additionally, it was demonstrated in a model of leukemia that alpha emitting nuclides display cytotoxicity that was able to break beta-irradiation-, gamma-irradiation-, doxorubicin-, and apoptosis-resistance [4]. There are a number of alpha particle-emitting nuclides considered for application in targeted therapy displaying half-lives ranging from minutes to days. ^{213}Bi is one alpha particle-emitting nuclide ($t_{1/2}$ = 46 min) that has been proposed for therapeutic use and has been evaluated clinically. However, ^{213}Bi is generator-produced, has a very short half-life and presents a logistical dilemma of eluting the generator, radiolabeling the targeting molecule, administering a dose, and allowing sufficient time for targeting. All of these steps consume valuable time that decreases the effective dose administered. An alternative to ^{213}Bi was to utilize its parent nuclide, ^{225}Ac, which has a ten-day half-life and 4 net alpha particle-emissions per decay (Figure 1). In vitro cytotoxicity data using the same antibodies labeled with either ^{213}Bi or ^{225}Ac demonstrated that several logs less ^{225}Ac radioactivity was required to reach LD_{50}, presumably because of the longer half-life and multiple alpha emissions [5]. The enhanced potency of ^{225}Ac versus ^{213}Bi was also demonstrated in vivo in a model of prostate cancer [5, 6]. This article reviews the literature of ^{225}Ac dealing with its production and supply, physical, chemical and biological properties, dosimetry, and clinical use as a radiotherapeutic agent in cancer therapy.

2 ^{225}Ac Production and Supply

The actinium nomenclature was derived from the Greek *aktis* or *aktinos*, meaning ray or beam [7]. The element was discovered by Andre Louis Debierne in 1899 and independently by Friedrich Oskar Giesel in 1902 [8]. Actinium occurs naturally in association with uranium radionuclides and ^{225}Ac can be obtained either from the decay of ^{233}U or from the neutron transmutation of ^{226}Ra by successive n,γ capture decay reactions *via* ^{227}Ac, ^{228}Th to ^{229}Th [9–11]. Currently, there are two sources of ^{225}Ac that have been used in clinical trials: (1) the U.S. Department of Energy, Oak Ridge National Laboratory (ORNL) in Oak Ridge, TN, United States of America and (2) the Institute for Transuranium Elements in Karlsruhe, Germany. The ^{225}Ac at both sites is derived from ^{233}U that was produced as a component of the U. S. molten salt breeder reactor program [12–14], which has been in long-term storage at ORNL. The bulk of the current high purity and low specific activity ^{229}Th was separated from waste material associated with the original production of the ^{233}U. This ^{229}Th yields ^{225}Ac that is produced as a “carrier-free” nuclide and is suitable for use in clinical research applications. The ^{225}Ac from both sources has been used to construct ^{213}Bi producing generators [15, 16] for Phase I and I/II clinical treatment of leukemia [17] and the ^{225}Ac from Oak Ridge used to directly radiolabel an antibody for application in a Phase I clinical trial treating leukemia (ongoing clinical trial, [18]).

An ^{225}Ac generator based on a design that adsorbed ^{229}Th oxide onto a titanium phosphate resin was described by Geerlings *et al.* [19]. Elution of this ^{229}Th cow with dilute nitric acid yielded a mixture of radionuclides: ^{225}Ac, ^{225}Ra, and ^{224}Ra. Another downstream column, containing Dowex 50 WX8, was used to purify the ^{225}Ac by removing the ^{225}Ra, ^{224}Ra, and the ^{224}Ra decay products. In 1993, it was proposed that the ^{225}Ac thus produced could be used to label an antibody or be affixed to a resin as a parent for a ^{213}Bi generator product.

The steps for isolating ^{225}Ac from the ^{229}Th at Oak Ridge National Laboratory was described by Boll and Mirzadeh *et al.* [14]. In the initial process design, the ^{229}Th, ^{225}Ra, and ^{225}Ac reach equilibrium in 45 days and carrier-free ^{225}Ra and ^{225}Ac were separated from the thorium stock in nitric acid using anion exchange chromatography with a Reillex HPQ resin. Concentration of the ^{225}Ra /^{225}Ac eluate was effected by evaporation or neutralization and co-precipitation. Recently, this group has described a four-step chemical separation procedure, employing both anion and cation exchange chromatography, to process their current supply of 150 mCi of ^{229}Th into ^{225}Ac [13]. Over an 8-week period, approximately 100 mCi of ^{225}Ac is yielded per processing campaign and the product shipped in 5–6 batches. Following the initial process run of a campaign yielding ~ 50–60 mCi ^{225}Ac, the radium pool is reprocessed biweekly to yield the additional ^{225}Ac shipments. This material is currently being utilized in both a ^{213}Bi- and an ^{225}Ac-labeled antibody trial at Memorial Sloan-Kettering Cancer Center (MSKCC) [17]. The average radionuclidic purity is 99.6% ± 0.7% ^{225}Ac with ≤ 0.6% ^{225}Ra contaminant and an average ^{229}Th content of $4\ (+5/-4) \times 10^{-5}$ %.

The method for separation and purification of ^{225}Ac from a ^{229}Th source that is currently employed at the Institute for Transuranium Elements was described by Apostolidis *et al.* [12]. The ^{229}Th stock was batch loaded in nitric acid onto 0.5 L of Dowex 1×8 anion exchange resin. Their process utilizes a combination of extraction and ion exchange chromatographic methods to obtain carrier-free, clinical quality ^{225}Ac with > 95% overall yield. Based upon their stock of 215 mg of ^{229}Th, they can isolate 43 mCi of ^{225}Ra and 39 mCi of ^{225}Ac every 9 weeks. This ^{225}Ac has been used in clinical generators [16] to produce ^{213}Bi for radiolabeled radioimmunopharmaceuticals at MSKCC [17] and in collaborations with a number of other sites [12].

A liquid ^{229}Th/^{225}Ac generator was proposed by Khalkin *et al.* [20] in a process that entails maintaining a stock ^{229}Th solution in an ammonium citrate solution in order to eliminate the radiolysis and degradation experienced with solid sorbents. As the ^{225}Ra and ^{225}Ac reach equilibrium with the ^{229}Th, they are isolated in a one-step cation exchange process. The ^{229}Th breakthrough is effectively removed in a single separation cycle by changing the pH of the solution. This process takes advantage of the differences in the stability constants of thorium ($K_1 = 10^{13}$, $K_2 = 10^8$) and actinium ($K_1 \sim K_2 = 106$) citrate complexes [21].

An alternate strategy to ^{225}Ac production employs proton irradiation of ^{226}Ra which can lead to ^{225}Ac *via* [p,2n] reactions [9, 10, 22] using a cyclotron. Theoretically, the irradiation of 1 mg of ^{226}Ra should yield approximately 35 mCi of ^{225}Ac [10]. Recently, the feasibility of cyclotron produced ^{225}Ac was demonstrated and maximum yields were reached with an incident proton energy of 16.8 MeV [22] using the ^{226}Ra(p,2n)^{225}Ac reaction. In this work, 0.0125 mg of ^{226}Ra yielded 0.0021 mCi ^{225}Ac after irradiation of a 36 mm^2 target with a 10 μA proton current for 7 h. No significant differences were found in the radionuclidic purity of the cyclotron product when compared to ^{225}Ac produced *via* the ^{229}Th method [12] and ^{213}Bi produced from this ^{225}Ac was found to label antibody constructs with approximately 90% yield.

3 Physical and chemical properties of ^{225}Ac

^{225}Ac produces six predominant radionuclide daughters in the decay cascade to stable ^{209}Bi [23]. A single ^{225}Ac ($t_{1/2}$ = 10.0 d; 6 MeV α particle) decay yields net 4 alpha and 3 beta disintegrations, most of high energy and 2 useful gamma emissions of which the ^{213}Bi 440 keV γ emission has been used in imaging drug distribution [17]. These daughters are ^{221}Fr ($t_{1/2}$ = 4.8 m; 6 MeV α particle and 218 keV γ emission), ^{217}At ($t_{1/2}$ = 32.3 ms; 7 MeV α particle), ^{213}Bi ($t_{1/2}$ = 45.6 m; 6 MeV α particle, 444 keV β^- particle and 440 keV γ emission), ^{213}Po ($t_{1/2}$ = 4.2 μs; 8 MeV α particle), ^{209}Tl ($t_{1/2}$ = 2.2 m; 659 keV β^- particle), ^{209}Pb ($t_{1/2}$ = 3.25 h; 198 keV β^- particle) and ^{209}Bi (stable). Given the 10.0 d half-life of ^{225}Ac, the large alpha particle emission energies, and the favorable rapid decay chain to stable ^{209}Bi this radionuclide was recognized as a potential candidate for use in cancer therapy [19].

The potential for using ^{225}Ac as a therapeutic radionuclide was limited for a number of years by the availability of suitable chelator moieties capable of stably binding the radionuclide as well as controlling the fate of the daughters [21]. In addition, the chemistry of actinium was not well explored or developed. Diamond and Seaborg [24] studied the elution characteristics of the transuranium elements in hydrochloric acid on cation-exchange resin and concluded that the actinides may form complex ions with chloride to a greater extent than the lanthanide elements. Their explanation was that there was a partial covalent character to the actinide bonds involving hybridization of the 5f orbitals. The actinium(III) ionic radius was reported as 0.111 nm [24]. Yamana *et al.* used the radiopolarographic reduction of ^{225}Ac(III) in aqueous solution in the presence of 1,4,7,13,16-hexaoxacyclooctadecane (18-CROWN-6) to argue the formation of a divalent actinium cation [25]. In the absence of 18-CROWN-6, the measured $E_{1/2}$ value was -2.15 V *versus* SCE and as increasing concentrations of 18-CROWN-6 were added, the $E_{1/2}$ value shifted to a more negative potentials in a linear fashion. They concluded from this study that the Ac(II) ionic radius was 0.125 nm and the electronic configuration was [Rn]6d^1. In order to address the issue of hydrolysis of ^{225}Ac in aqueous solution, Kulikov *et al.* [26] determined the overall hydrolytic constant, β_3, for the 225Ac(III) ion in aqueous $NaClO_4$ (μ = 0.1). They used the electromigration method in free electrolyte solution to investigate hydrolysis. A plot of the ^{225}Ac ion velocity as a function of pH shows a constant velocity of 5.4×10^{-4} cm^2/Vs in the pH interval from 4–10, indicating that no hydrolytic process occurs until pH = 10. At pH 10, the velocity drops steeply and by pH 11 the velocity is 0. A value of $p\beta_3$ = 31.9 ± 0.2 was calculated for the hydrolytic reaction, $Ac^{3+} + 3H_2O \rightarrow Ac(OH)_3 + 3H^+$, where β_3 is the hydrolytic constant. When the pH was < 4, a 10–15% decrease in ion mobility was measured; this phenomenon was not explained by the authors.

4 Biological studies

The initial work in this area was concerned with the biodistribution, metabolism and methods to alter the pharmacokinetics of ingested ^{227}Ac. ^{227}Ac is a nuclide in the ^{235}U decay scheme with a 21.77 y half-life and numerous alpha particle-emitting progeny [23]. Concerns regarding the radionuclidic progeny were noted but not fully addressed. However, when the potential for using ^{225}Ac as a tumoricidal agent was considered, complexing agents and chelates were sought to enhance tumor uptake and avoid normal organ uptake. ^{225}Ac complex stability improved by trial and error and a trend was recognized as one moved from simple complexing agents to acyclic chelates to macrocyclic chelates. Two related macrocyclic chelates, in particular, were identified as potentially useful and further explored as moieties to attach to targeting monoclonal antibody carriers. The first was 1,4,7,10,13,16-hexaazacyclohexadecane-*N,N′,N″,N‴,N⁗,N⁗′*-hexaacetic acid (HEHA) and the second was 1,4,7,10-tetraazacyclododecane-*N,N′,N″,N‴*-tetraacetic acid (DOTA).

These chelates are related because they are both macrocycles that present carboxylic acid and amine functionalities to the metal-ion, albeit with different denticity, macrocycle size, and overall charge. As will be described below, the ^{225}Ac complex with HEHA demonstrated less stability than the ^{225}Ac complex with DOTA *in vivo* in the experiments described. In addition, the two monoclonal antibody/antigen systems that were examined using HEHA-constructs were non-internalizing immune complexes and the targeted constructs could still release the daughters systemically. The ^{225}Ac released from the HEHA was distributed to liver and bone and the subsequent release of its daughters contributed to acute radiotoxicity as did the daughters from the targeted but not internalized parent. The ^{225}Ac complex formed with DOTA was considerably more stable *in vivo* and the antibodies selected for these studies formed internalizing immune complexes with their respective antigen targets.

The isothiocyanate-functionalized derivatives of DOTA were selected as the most promising to pursue for coupling to antibody molecules from out of a group of potential ^{225}Ac chelate compounds: diethylenetriaminepentaacetic acid (DTPA), 1,4,8,11-tetraazacyclotetradecane-1,4,8,11-tetraacetic acid (TETA), DOTA, 1,4,7,10-tetraazacyclododecane-1,4,7,10-tetrapropionic acid (DOTPA), 1,4,8,11-tetraazacyclotetradecane-1,4,8,11-tetrapropionic acid (TETPA), and 1,4,7,10-tetraazacyclododecane-1,4,7,10-tetramethylenephosphonic acid (DOTMP). The bifunctional chelating agents MeO-DOTA-NCS, (α-(5-isothiocyanato-2-methoxyphenyl)-1,4,7,10-tetraazacyclododecane-1,4,7,10-tetraacetic acid and 2B-DOTA-NCS, 2-(*p*-isothiocyanatobenzyl)-1,4,7,10-tetraazacyclododecane-1,4,7,10-tetraacetic acid were both evaluated and compared as their respective [^{225}Ac]DOTA-antibody construct. A two-step labeling method was developed using several different IgG systems [27]. The chelation reaction yield in the first step was 93% ± 8% radiochemically pure (n = 26). The second step which couples the [^{225}Ac]DOTA-SCN moiety to the IgG, yielded constructs that were 95% ± 5% radiochemically pure (n = 27) and with mean percent immunoreactivity ranging from 25% to 81%, depending on the antibody used but consistent for each IgG system. This methodology met the requirement for high temperature labeling of the DOTA chelate with ^{225}Ac without sacrificing the biological activity of the protein.

Subsequently, animal xenograft models of human cancers could effectively be treated with single or multiple doses of [^{225}Ac]DOTA-IgG with no acute systemic radiotoxicity since the pharmacokinetic fate of the ^{225}Ac was tied to the targeting protein. A number of studies using the DOTA constructs followed which investigated other antibody-antigen systems, selective T-cell ablation, and studies aimed at discovering methods to control ^{225}Ac and the pharmacokinetics of the daughters. This work has culminated in the initiation of a Phase I clinical trial using the construct [^{225}Ac]DOTA-HuM195 directed against leukemia.

4.1 Actinium biodistribution and metabolism in rodents

In 1970 Taylor examined the biodistribution and metabolism of ^{227}Ac in a male rat model [28]. While, this study concerned ^{227}Ac, a member of the ^{235}U decay scheme and not ^{225}Ac, it did address the *in vivo* distribution and sub-cellular metabolism of actinium metal-ion and brings up the issue of the independent distribution of its daughters. Taylor performed intraveneous injections of 18.5 kBq (500 nCi) of ^{227}Ac nitrate solution mixed with serum proteins from isologous rat serum, nitrate ion, 1% sodium citrate or 0.5% sodium diethylenetriaminepentaacetic acid. The pH of these solutions was adjusted to 6.5. The liver was the primary site for ^{227}Ac localization and at 4 d post injection, ^{227}Ac was found to be associated with lysozymes in the subcelluar fraction of the liver. 40% of the injected dose of ^{227}Ac-serum protein was excreted in 28 d, and the remainder cleared the rat with a $t_{1/2}$ of 700d. DTPA used as a rescue agent for ^{227}Ac contamination was capable of effecting a 60% reduction in the body burden, but only if administered within 30 minutes of exposure.

Transferrin was implicated as the serum protein involved in sequestering and transporting the ^{227}Ac *in vivo*. Several other references to the metabolism and biodistribution of ^{227}Ac appear in the literature [29–32] but are not reviewed herein.

In 1990, the biodistribution of a mixed ^{225}Ac, ^{169}Yb and ^{148}Pm (1:3:0.3) isotonic sodium citrate solution, adjusted to pH 6.5, was examined in normal male Wistar rats and female C_3H SPF mice bearing mama adenocarcinoma tumor implants by Beyer *et al.* [33]. The rats were injected i.v. while the mice were injected i.p. Each animal received 40 kBq (1080 nCi) of ^{225}Ac in a citrate solution. Animals were sacrificed 5 h post-injection and blood, liver, femur, urine, and tumor (in the mice) were harvested. Samples were measured one day after harvest using a high resolution Ge(Li)-spectrometer after secular equilibrium was established. As expected for a rapidly clearing metal-citrate complex, the %ID ^{225}Ac /g of blood was low, 0.06 and 1.2 for rats and mice, respectively. Inter-species liver and femur values were very different, however, the rats had 5.7 and 1.18 %ID ^{225}Ac /g while the mice had 38.7 and 16.8 %ID ^{225}Ac /g, respectively. Tumor in mice accumulated 3.54 %ID ^{225}Ac /g.

The influence of varying ethylenediamine-tetramethylenephosphonic acid (EDTMP) solution concentrations on the biodistribution of ^{225}Ac and radiolanthanides was determined in tumor-bearing mice [34]. Female Swiss nu/nu mice were implanted with subcutaneous T380 human colon carcinoma and injected intraveneously *via* the tail vein with approximately 50 kBq ^{225}Ac (1350 nCi) in formulations varying the concentration of EDTMP (0, 0.01, 0.05, 0.1, 0.2, 0.5, 1, 2, 10 and 30 mM) or in a 1 mM citrate control solution, adjusted to pH 6.5. Animals were sacrificed at 15 hours and blood, liver, femur, urine, muscle, spleen, tumor, kidney, fat, and heart were harvested and measured using a high resolution Ge-spectrometer after secular equilibrium was established. [^{225}Ac]citrate control and [^{225}Ac]EDTMP solutions (up to 0.1 mM EDTMP) demonstrated high liver uptake (40 %ID/g). At higher EDTMP concentrations (30 mM EDTMP) less than 1 %ID/g ^{225}Ac accumulated in the liver. The excess EDTMP assisted the clearing of the ^{225}Ac.

The biodistribution, dosimetry and radiotoxicity of ^{225}Ac complexed with acetate, ethylenediaminetetraacetic acid (EDTA), 1,4,7,10,13-pentaazacyclopentanadecane-*N,N′,N″,N‴, N⁗*-pentaacetic acid (PEPA), and the A″ isomer of *N*-[(*R*)-2-amino-3-(4-nitrophenyl)propyl]-*trans*-(*S,S*-cyclohexane-1,2-diamine-*N,N,N′,N″,N⁗*-pentaacetic acid (CHX-A″-DTPA) was examined in female BALB/c mice by Davis *et al.* [35]. Animals were sacrificed at 1h, 4h, 24h, 5d, and 8d following intraveneous tail vein injection of 92 kBq (2500 nCi) of each of the ^{225}Ac complexes in MES buffer. Tissue samples (skin, muscle, femur, uterus/ovaries, stomach, jejunem, ascending colon, liver, kidney, spleen, sternum, thymus, heart, lung and 0.010 mL whole blood) were harvested, held for 4 hours, and then counted using a NaI(Tl) γ-scintillation counter. Data expressed as the %ID/g again demonstrated that the liver is the major site of ^{225}Ac localization for all four small molecule complexes studied. Liver accumulation increases according to the decreasing strength of the ^{225}Ac-complex: CHX-DTPA ~ PEPA > EDTA > acetate. For example, the 24h liver biodistribution data values were approximately 13, 15, 53, and 110 %ID/g for the respective [^{225}Ac]CHX-DTPA, [^{225}Ac]PEPA, [^{225}Ac]EDTA, ^{225}Ac-acetate complexes. When the data were expressed as the % injected dose per organ it was shown that for [^{225}Ac]CHX-DTPA, the bone is the predominant site of localization and the liver next (at 24 h, 42 %ID/bone and 13 %ID/liver). Liver and femur accumulation presumably result from the leakage of ^{225}Ac from the chelators.

Absorbed dose values for ^{225}Ac were estimated based upon the data from [^{225}Ac]CHX-DTPA and [^{225}Ac]EDTA. Values are reported as Gy per 92 kBq of injected dose of ^{225}Ac-

complex. For [^{225}Ac]CHX-DTPA and [^{225}Ac]EDTA the doses to liver were 30.4 and 117.8; 7.8 and 15.4 to bone; and 3.2 and 2.1 to kidney, respectively [35].

Both acute and chronic toxicity were assessed by organ system damage and white blood cell (WBC) counts as a function of the dose administered. Two mice receiving 92, 185, 370, 740 kBq (2,500, 5,000, 10,000, 20,000 nCi) of [^{225}Ac]CHX-DTPA were sacrificed at days 2, 5, 7, 53 post-injection (the latter two timepoints were included for animals that had not succumbed to radiation toxicity during the study). The control was i.v. injected CHX-DTPA chelate-alone in MES buffer. Tissues from these animals were harvested, hematoxylin and eosin stained and fixed, evaluated histopathologically, and graded for radiation damage. The organs that showed the most evidence of radiation-induced toxicity were the bone marrow, spleen, gastrointestional tract, and the liver. At the 92 kBq dose level, the WBC, spleen and bone marrow were rated as having loss of cellular numbers, integrity, orientation, or structure. At the 185 kBq dose level the WBC, spleen, bone marrow, liver, GI tract, and kidney all were rated as having loss of cellular numbers, integrity, orientation, or structure and evidence of cellular necrosis [35].

Another series of ^{225}Ac-labeled chelate complexes was prepared and their biodistribution measured in normal BALB/c mice by Deal *et al.* [36]. One of these complexes was reported to exhibit improved *in vivo* stability relative to the others in the series examined. The chelates included EDTA, CHX-A-DTPA, PEPA, DOTA, HEHA, and acetate. 92.5 kBq of each complex (2500 nCi) in MES buffer at pH 6.2 was injected into normal female BALB/c mice *via* the tail vein. Biodistributions were performed at 1, 4, 24, 120 h and samples were counted after 4 h to allow for secular equilibrium. All of the complexes rapidly cleared the blood with < 2 %ID/g in 1 h. The order of most ^{225}Ac distributed into tissue to the least was acetate > EDTA > CHX-A″-DTPA ~ PEPA > DOTA > HEHA. Consistent with the studies described above, the loss of ^{225}Ac from an acyclic chelate is greatest and reflected in the high uptake in liver and bone and poor whole body clearance. [^{225}Ac]HEHA was rapidly excreted within 1 h and only 0.17 % ID/g remained (approximately 100 nCi of the 2500 nCi injected).

4.2 Monoclonal antibodies as targeting carrier molecules

The *in vitro* cytotoxicity of an [^{225}Ac]DTPA-antibody construct was reported by Kaspersen *et al.* using a murine IgG1 that targets a carbohydrate structure associated with the EGF receptor expressed on the human epidermoid A431 tumor cell line [37]. It was noted that the specific antibody construct was more potent than the non-specific control construct. However, the DTPA chelate moiety was clearly not able to stably bind the ^{225}Ac in these experiments as demonstrated by the ^{225}Ac constructs being capable of killing target cells only slightly better than similarly labeled ^{213}Bi-antibodies.

In addition to the series of ^{225}Ac-labeled chelate complexes that were studied the biodistribution of an antibody carrier molecule was also examined [36]. The antibody 201B targets and binds to mouse lung endothelial thrombomodulin and was chemically coupled with CHX-A-DTPA to yield a DTPA-201B construct that was radiolabeled with ^{225}Ac. The [^{225}Ac]DTPA-201B construct efficiently targeted the lung but the ^{225}Ac had a very short tissue $t_{1/2}$ of 4–5 h as compared with the [^{125}I]201B construct with a $t_{1/2}$ of 4–5 d. The DTPA was unable to stably bind the ^{225}Ac at the site *in vivo*.

HEHA is a multidentate, macrocyclic chelate having 6 carboxylic acids and 6 amino nitrogens (compare with PEPA having 5 of each and DOTA having 4 of each). The larger macrocycle size, greater number of coordinating ligands, and overall negative 3 charge of the [^{225}Ac]HEHA complex were hypothesized to mediate the enhanced clearance relative to the other chelates. These properties were useful for the simple complex *in vivo*, but did not

address the potential stability should the HEHA chelate be used in an IgG construct that would presumably have a longer biological half-life [36]

The interest in the HEHA chelate led to the description of the synthesis of the isothiocyanate derivative, the conjugation to three different antibodies, and radiolabeling of with ^{225}Ac by Chappell *et al.* [38]. One of the [^{225}Ac]HEHA-IgG constructs was evaluated for serum stability in fetal bovine serum at 37°C over a 3 day period. After 0.4 h of incubation, 99% of the ^{225}Ac was still associated with the construct, but at 1, 3, 5, 24, and 48 h this value rapidly decreased to 77, 73, 69, < 50, and < 50%, respectively. It was determined that free ^{225}Ac will associate and bind rapidly and quantitatively to serum proteins.

The [^{225}Ac]HEHA-201B antibody construct was evaluated for vascular targeted therapy of lung tumors in the first reported radiotherapeutic study of ^{225}Ac *in vivo* by Kennel and co-workers [39]. This study performed biodistribution, dosimetry and therapeutic efficacy studies in female BALB/c mice with the EMT-6 mammary carcinoma as the model. At 1 and 4 h post-injection, 300 %ID/g of ^{225}Ac was distributed to the target lung, however the ^{225}Ac cleared the lung with a $t_{1/2}$ of 49 h. The ^{225}Ac released from the HEHA accumulated predominantly in the liver, spleen, and bone. It was calculated that a 6 Gy per microCurie dose was delivered to the lungs and about three-fold less to other tissues. A therapeutic study was performed where 18.5 kBq of construct administered per mouse allowed 10% of the tumored-animals to survive 23 d vs. 11 to 15 d for untreated controls. 80% of the animals treated with 37 kBq of ^{225}Ac drug had the tumor eradicated but died at 16 d from acute radiotoxic effects (total bone marrow abalation, splenic atrophy, damage to the lining of the stomach and intestine). In subsequent studies, no therapeutic window could be identified that would effectively treat tumor but spare the host. The leakage of the ^{225}Ac from the HEHA chelate and the non-internalizing antibody-antigen complex compromised the use of this system for radioimmunotherapy.

4.2.1 The targeting Nanogenerator approach—A strategy whereby the therapeutic potential of ^{225}Ac could be harnessed would by necessity require controlling the fate of the parent and the several radionuclidic progeny. As will be described below, early studies sought to determine suitable chelating agents that would yield stable ^{225}Ac complexes *in vivo* and thereby shape the pharmacokinetic profile of the parent nuclide by keeping the parent nuclide associated with the targeting carrier immunoglobulin. Managing the distribution, metabolism and clearance of the daughters was a more daunting task. Some attempts were focused on developing a single chelate moiety to accommodate the parent and the daughters, however, that task proved difficult given the range of different periodic properties of these daughters. The approach which was taken by McDevitt *et al.* [5] focused on i) stably chelating the ^{225}Ac for delivery *in vivo* to a target cell; ii) internalizing the ^{225}Ac-antibody construct into the target cell; iii) retaining the progeny and decay products within the target cell and harnessing their cytotoxic potential; and iv) reducing the loss of the daughters to non-target tissues and mitigating systemic radiotoxic events. This latter strategy was called the ^{225}Ac nanogenerator system (Figure 2). A stable DOTA chelate for ^{225}Ac was identified as was a robust thiourea chemical linkage between the chelate and the targeting carrier molecule. Targeting agents such as internalizing IgGs transported the ^{225}Ac into the cell where decay daughters were retained if the drug was internalized. This approach proved extremely cytotoxic to the targeted cancer cells and limited the systemic toxicity to the host. The ^{225}Ac delivered to the cancer cell was effectively a therapeutic nanogenerator of multiple alpha particle emissions within the target cell [5].

The first practical application of ^{225}Ac in targeted drug therapy without accompanying systemic radiotoxicity utilized the nanogenerator approach [5]. This process was dependent on the stable chelation of the parent ^{225}Ac radionuclide and the efficient delivery and

internalization of the construct at the tumor target site. Controlling the [^{225}Ac]DOTA-antibody pharmacology was the key to the use of ^{225}Ac as a therapeutic agent. Further, retaining the daughters at the target site and harnessing their cytotoxic potential contributed to safe and effective tumor therapy with targeted atomic nanogenerators. It was discovered that a very stable ^{225}Ac complex with DOTA could be rapidly formed at 60°C. The ensuing [^{225}Ac]DOTA complex could then be coupled to an IgG using a thiourea linkage [27]. Figure 3 contains normal murine biodistribution data at 24 hours for ^{225}Ac-acetate, [^{225}Ac]DOTA-SCN, and the antibody construct, [^{225}Ac]DOTA-HuM195.

The stability *in vitro* of [^{225}Ac]DOTA-HuM195 was compared to [^{177}Lu]DOTA-HuM195, in 100% human serum, 100% mouse serum, and 25% human serum albumin at 37°C for 15 days. The [^{225}Ac]DOTA-HuM195 displayed stability similar to the ^{177}Lu analogue, with less than 5% loss of ^{225}Ac from the IgG over 15 days. The stability results in all three conditions were similar [5].

Stability *in vivo* was determined using 10 female nude mice injected i.v. with 300 nCi of [^{225}Ac]DOTA-HuM195. The % ^{225}Ac that was bound to the HuM195 in the mouse serum was determined as a function of time. IgG bound ^{225}Ac was determined using a Protein A binding assay, HPLC size exclusion chromatography analysis of the serum, and a cell based immunoreactivity fraction assay. The results of the Protein A bead assay at 5 timepoints from 2.5 to 120 hours, showed that the mean % ^{225}Ac that was bound to the HuM195 was 98.2 to 99.9%, respectively. HPLC analysis of the ^{225}Ac species in the serum also indicated that it was associated with the HuM195. The immunoreactivity assay of a serum sample indicated that 63% of the ^{225}Ac species was bound to CD33 expressing AL67 cells versus 3% bound to non-specific Daudi cells. In conclusion, ^{225}Ac bound to HuM195 remained associated with the IgG following injection into a mouse over a 5 d period, demonstrating the stability of the drug *in vivo* [5].

The *in vitro* cytotoxicity of ^{225}Ac-antibody constructs that were specific for HL60 leukemia cells (HuM195 (anti-CD33)); Daudi and Ramos lymphoma cells (B4 (anti-CD19)); MCF7 breast carcinoma cells (trastuzumab (anti-HER2/neu)); LNCaP.FGC prostate carcinoma cells (J591 (anti-PSMA)); and SKOV3 ovarian cancer cells (trastuzumab (anti- HER2/neu)) were examined using very small doses of nanogenerators. The LD_{50} values of the ^{225}Ac constructs ranged from 0.3 to 74 Bq/mL (0.008 to 2 nCi/mL) and were 2–4 orders of magnitude lower than values for corresponding ^{213}Bi alpha-particle emitting antibodies (approximately 7400 Bq/mL). Controls at low specific activities (accomplished by adding excess unlabeled antibody) did not show specific binding of the alpha-particle generators to the targets, and were used to represent non-specific cytotoxicity. The LD_{50} values were 10- to 625-fold higher in the controls using excess unlabeled antibody [5]. Some representative data are presented in Table I to compare the LD_{50} values of ^{225}Ac and ^{213}Bi labeled antibody constructs that targeted the same cancer cell lines with the same antibodies.

A pharmacokinetic analysis of the ^{225}Ac construct and two of its daughters was performed *in vivo* by injecting 12 kBq of [^{225}Ac]DOTA-J591 or 12 kBq of [^{225}Ac]DOTA-HuM195 (irrelevant control) i.p. in two groups of male athymic nude mice (n=12 per group) bearing a 3–4 week old LNCaP i.m. tumor xenograft. Approximately, 18 and 21 %ID/g of [^{225}Ac]DOTA-J591 was localized in the tumor at 2 and 3 days, respectively. Tumor samples (average ± S.D., $n \geq 3$) counted 6 - 12 min. after sacrifice/harvest, demonstrated that ^{221}Fr was 88% ± 9% and ^{213}Bi was 89% ± 2% of the ^{225}Ac secular equilibrium levels in the tumor. These results indicate the uptake of the parent IgG construct by the tumor and the subsequent retention of the daughters at that location [5].

In toxicity experiments, the maximum tolerated dose (MTD) in 20 g naive mice was 18.5 kBq (500 nCi) [^{225}Ac]DOTA-IgG. Mice injected with 37 kBq (1000 nCi) of [^{225}Ac]IgG died. Based on these studies, therapeutic doses were selected that were approximately 40% of MTD [5].

To investigate the therapeutic efficacy *in vivo* of the generator construct, [^{225}Ac]DOTA-J591, an intramuscular (i.m.) LNCaP tumor model in male nude mice was utilized. Serum prostate specific antigen (PSA) is an important surrogate marker for prostate cancer burden and prognosis in humans and was utilized in this xenograft model to follow tumor growth. The experimental groups of animals had mean PSA values of 2–5 ng/mL on 10 and 12 days after implantation of tumor. At the time the [^{225}Ac]DOTA-J591 was administered on day 12 or 15, the tumors were characterized histologically as vascularized and encapsulated nodules each comprised of tens of thousands of cells. Animals were sacrificed when tumor area was ≥ 2.5 cm^2.

In the first therapy experiment, male nude mice ($n = 13$) were treated on day 15 post-tumor implantation and received 7.2 kBq [^{225}Ac]DOTA-J591 in a single nontoxic administration. These animals had significantly improved ($P < 0.006$) median survival times relative to mice treated with a similar dose of [^{225}Ac]DOTA-B4 irrelevant control antibody mixed with unlabeled specific J591 (dual control) or untreated controls. There was no significant difference in survival times between the dual control-treated animals and untreated controls. The median survival time of untreated growth controls in this model was 33 days ($n = 15$). The mean and median pre-therapy PSA values measured on day 12 were not significantly different between the three groups of mice. However, on days 28 and 42, the PSA values of [^{225}Ac]DOTA-J591 treated animals were significantly lower than the PSA values for the dual control-treated animals and untreated controls. There was no significant difference between the dual control-treated animals and untreated controls at either time. Additionally, no acute radiotoxicity was observed [5].

In a second experiment, mice ($n = 39$) were treated on day 12 after LNCaP tumor implantation with a single, non-toxic administration of 7.8 kBq [^{225}Ac]DOTA-J591 which caused tumor regression and significantly improved ($P < 0.0001$) the median survival times of these mice to 158 days compared to the 63 days in the mice treated on day 15. PSA values decreased from pre-therapy levels in many of the animals following treatment to low and undetectable levels and remained undetected in the 14 of the 39 treated animals which exhibited prolonged survival. These mice survived at least 10 months and had no measureable PSA or evidence of tumor at the time of sacrifice (293 days). Animals treated with unlabeled J591 (0.004 or 0.04 mg) on day 12 post-implantation had no prolongation of median survival (37d and 35d, respectively, $n = 9$). The therapeutic efficacy was dependent on antibody specificity, the administration of the ^{225}Ac-generator, and the treatment time after implantation [5].

In order to determine if other tumor types could be treated with ^{225}Ac-generator constructs, a disseminated human Daudi lymphoma cell mouse model using [^{225}Ac]DOTA-B4 as the therapeutic agent was investigated. Female SCID mice were treated 1 day after tumor dissemination with a single administration of specific [^{225}Ac]DOTA-B4 (three different dose levels), irrelevant control [^{225}Ac]DOTA-HuM195 (two dose levels), or unlabeled B4. Control mice receiving the irrelevant [^{225}Ac]DOTA-HuM195 had median survival times from xenograft of 43 days (5.6 kBq) and 36 days (1.9 kBq). Mice receiving 0.003 mg unlabeled B4 per mouse had a median survival time of 57 days. The mice receiving a single injection of [^{225}Ac]DOTA-B4 showed dose-related increases in median survival times 165 (6.3 kBq), 137 (4.3 kBq), and 99 days (2.1 kBq), respectively. This dose response of

[^{225}Ac]B4 was significant with $P = 0.05$. About 40% of mice treated at the highest dose were tumor-free at 300 days and the experiment concluded on day 310 [5].

The time of treatment from tumor implantation was examined in the second disseminated lymphoma experiment *in vivo*. Mice ($n = 15$) that received treatment on day 1, 3, or 6 post tumor implantation with a single administration of [^{225}Ac]DOTA-B4 (6.3 kBq) had similar prolongation of survival relative to untreated growth controls. Mice ($n = 5$) that received treatment 13 days after tumor dissemination survived > 165d. Unlabeled B4 was minimally active in mice ($n = 5$ per group) with median survival of 44 days and 40 days for mice treated with 0.002 mg or 0.20 mg, respectively. Untreated growth controls ($n = 15$) had a median survival time of 28 days. Therefore, in this lymphoma model, while specificity and dose level were important factors in efficacy, the treatment time after tumor dissemination was less relevant up to a time-point, at which it was then inversely related to activity. The latter phenomenon may be related to differences in the geometry of the alpha emission eradicating single cells or clusters of tumor cells [5].

Previous workers have concluded that ^{225}Ac-antibody constructs were too unstable and that the daughters present an untenable pharmacological problem. The findings [5], demonstrated the ability to safely and efficaciously use ^{225}Ac as a stable and extraordinarily potent tumor-selective molecular sized generator in both established solid carcinomas or disseminated cancers.

Following these initial studies, the same strategy was employed in an i.p. radioimmunotherapy experiment in a mouse model of human ovarian cancer using ^{225}Ac labeled trastuzumab, an anti-HER-2/neu antibody, by Borchardt et al. [40]. The construct was prepared using the two-step methodology [27] and the radioimmunoconjugate was tested for immunoreactivity, internalization and cytotoxicity *in vitro* using a human ovarian carcinoma cell line, SKOV3. [^{225}Ac]DOTA-trastuzumab retained immunoreactivity (50–90%), rapidly internalized into cells (50% at 2 h) and had an ED_{50} of 1.3 nCi/mL. Intraperitoneal administered [^{225}Ac]DOTA-trastuzumab had a high tumor uptake, 60 %ID/g at 4 h. Tumor uptake was 3–5-fold higher than liver and spleen, the normal organs with the highest uptake. Therapy was examined with native trastuzumab and doses of 220, 330 and 450 nCi of [^{225}Ac]DOTA-trastuzumab or [^{225}Ac]DOTA-labeled control antibody at different dosing schedules. Therapy was initiated 9 days after tumor seeding. Groups of untreated control mice and those administered native trastuzumab had median survivals of 33 and 44 days, respectively. Median survival was 52–126 days with [^{225}Ac]DOTA-trastuzumab at various doses and schedules and 48–64 days for [^{225}Ac]DOTA-labeled control IgG. Deaths from radiotoxicity occurred with only the highest activity levels administered, the other dose levels were safe. It was concluded that i.p. administration with an internalizing [^{225}Ac]DOTA-labeled anti-HER2/neu antibody could significantly extend survival in a nude mouse model of human ovarian cancer at levels that produce no apparent gross toxicity.

Miederer and co-workers described the pharmacokinetics, dosimetry and toxicity of [^{225}Ac]DOTA-HuM195 in cynomolgus monkeys [41]. The monoclonal antibody, HuM195 (anti-CD33), was the targeting molecule intended for human clinical trials of [^{225}Ac]DOTA-IgG directed against leukemia. In one experiment, two monkeys received a single i.v. dose of [^{225}Ac]DOTA-HuM195 at 28 kBq/kg. This dose level was approximately that planned for initial human dose. In another experiment, two animals received a dose escalation schedule of three increasing [^{225}Ac]DOTA-HuM195 doses with a cumulative activity of 377 kBq/kg. There are no CD33 sites in cynomolgus monkeys and thus no targets for this antibody in this system. The construct was prepared using the two-step methodology [27].

Whole blood half-life of [^{225}Ac]DOTA-HuM195 construct; the ratio of ^{225}Ac:^{213}Bi; the generation of monkey anti-HuM195 antibodies (MAHA); haematological indices; serum biochemistries; and clinical observation were the parameters that were measured. Monkeys were euthanized and examined histopathologically when the dose escalation reached toxicity [41].

The blood half-life of [^{225}Ac]DOTA-HuM195 was 12 days and 45% of generated ^{213}Bi daughters were cleared from the blood. MAHA production was not detected. A dose of 28 kBq/kg of ^{225}Ac caused no toxicity at 6 months, whereas a cumulative dose of 377 kBq/kg caused severe toxicity. In the cumulative dosing schedule experiment, single doses of about 37 kBq/kg resulted in no toxicity at six weeks. After approximately 130 kBq/kg was administered, no toxicity was observed for 13 weeks. However, 28 weeks after this second dose administration, mild anemia and increases of blood urea nitrogen (BUN) and creatinine were detected. Following administration of an additional 185 kBq/kg, toxicity became clinically apparent. Monkeys were euthanized 13 and 19 weeks after the third dose administration (cumulative dose was 377 kBq/kg). Histopathological evaluation revealed mainly renal tubular damage associated with interstitial fibrosis [41].

In conclusion, ^{225}Ac nanogenerator constructs may result in renal toxicity and anemia at high doses. The longer blood half-life and the lack of target cell antigens in cynomolgus monkeys may increase toxicity compared to human application. It was concluded that a dose level of at least 28 kBq/kg may be a safe starting dose in humans, and that hematologic and renal function will require close surveillance during clinical trials.

The treatment of neuroblastoma meningeal carcinomatosis with intrathecal (i.t.) application of [^{225}Ac]DOTA-3F8 construct targeting ganglioside GD2 was evaluated by Miederer *et al.* using the nanogenerator approach [42]. 3F8 is an antibody that specifically binds to ganglioside GD2, overexpressed by many neuroendocrine tumors including neuroblastoma (NB). The [^{225}Ac]DOTA-3F8 construct was prepared using the two-step methodology [27] and was evaluated for radiochemical purity, sterility, immunoreactivity, cytotoxicity *in vitro*, induction of apoptosis on GD2-positive cells, as well as pharmacologic biodistribution and metabolism of the ^{225}Ac generator and its daughters in a nude mouse xenograft model of NB. Therapeutic efficacy was examined in a nude rat xenograft model of meningeal carcinomatosis and toxicity in cynomolgus monkeys after i.t. administration.

[^{225}Ac]DOTA-3F8 displayed radiochemical purity > 90%; an immunoreactivity of 65% in a cell-based immunoreactivity assay; an LD_{50} of 3 Bq/mL (80 pCi/mL) on the neuroblastoma cell line NMB7 *in vitro*; and it was shown to target specifically. Apoptosis of these cells was not observed. Biodistribution in mice showed specific targeting of a subcutaneous tumor with redistribution of the ^{225}Ac daughter nuclides mainly from blood to kidneys and to small intestine. In an extremely aggressive nude rat xenograft model of meningeal carcinomatosis, [^{225}Ac]DOTA-3F8 treatment i.t. improved survival time two-fold ($p = 0.01$). Increasing the construct specific activity to > 1 MBq/mg improved the therapeutic efficacy relative to lower specific activity preparations. Monkeys injected i.t. with multiple doses of the [^{225}Ac]DOTA-3F8 prepared under clinical manufacturing conditions, did not show any signs of toxicity based on blood chemistry and by complete blood counts or by clinical examination.

The efficacy of [^{225}Ac]DOTA-trastuzumab was determined against breast cancer spheroids with different HER2/*neu* expression levels by Ballangrud *et al.* [43]. The breast carcinoma cell lines MCF7, MDA-MB-361, and BT-474 with relative HER2/*neu* expression (expression level was determined by flow cytometry) of 1:4:18 were used. Spheroids of

these cell lines were incubated with different concentrations of [^{225}Ac]DOTA-trastuzumab, and spheroid growth was measured by light microscopy over a 50-day period.

The activity concentration required to yield a 50% reduction in spheroid volume at day 35 was 18.1, 1.9, and 0.6 kBq/mL (490, 52, 14 nCi/mL) for MCF7, MDA, and BT-474 spheroids, respectively. MCF7 spheroids continued growing but with a 20–30 day growth delay at 18.5 kBq/mL. MDA-MB-361 spheroid growth was delayed by 30–40 days at 3.7 kBq/mL and at 18.5 kBq/mL, 12 of 12 spheroids disaggregated after 70 days and cells remaining from each spheroid failed to form further colonies. Eight of 10 BT-474 spheroids failed to regrow at a concentration of 1.85 kBq/mL. All of the BT-474 spheroids at activity concentrations 3.7 kBq/mL failed to regrow and to form colonies. The radiosensitivity of these three cell lines evaluated as spheroids was described as the activity concentration required to reduce the treated-to-untreated spheroid volume ratio to 0.37, denoted DVR_{37}. The external beam radiosensitivity for spheroids of all three cell lines was found to be 2 Gy. After α-particle irradiation a DVR_{37} of 1.5, 3.0, and 2.0 kBq/mL was determined for MCF7, MDA-MB-361, and BT-474, respectively.

^{225}Ac-labeled E4G10 targeted the monomeric form of vascular endothelial cadherin in developing neovasculature [44, 45]. Treatment with 1.85 kBq (50 nCi) [^{225}Ac]DOTA-E4G10 on day 3, 5, 7 and 10 after xenotransplant of LNCaP prostate carcinoma cells achieved highly significant inhibition of tumor growth and lower PSA values 22 days after tumor implantation over [^{225}Ac]DOTA-non-specific IgG and vehicle. The lack of binding to tumor cells and to normal vasculature was demonstrated by flow cytometry, by SPECT imaging and by biodistribution studies. Additionally, subsequent bi-weekly administration of paclitaxel for two weeks resulted in further enhancement of the anti-tumor response to survival times of 182 days, compared to [^{225}Ac]DOTA-E4G10 monotherapy (113 days) and to combination of ^{225}Ac-labeled unspecific IgG with paclitaxel (84 days). The authors concluded that targeting the neovasculature with alpha particles was an effective approach to cancer therapy and that sequential therapy with chemotherapy could potentially result in a synergistic effect when temporal administration was carefully planned.

4.3 Other targeting modalities

4.3.1 Tetramers for specific CD 8 T-cell ablation—Major histocompatibility complex (MHC) tetramers are multimeric complexes capable of binding to specific CD8 T-cell clones and the targeted deletion of T-cell clones was examined using ^{225}Ac-MHC tetramers [46]. These molecules were conjugated to ^{225}Ac using a streptavidin platform to create an agent for CD8 T-cell clonal deletion. The ^{225}Ac-MHC tetramers specifically bound to, killed, and reduced the function of their cognate CD8 T cells while leaving the nonspecific control CD8 T-cell populations unharmed. The LMP1 peptide component confers T-cell specificity as the Flu peptide confers non-specificty. Biotinylated DOTA was prepared and labeled with ^{225}Ac in high yield (≥ 96%).

The ^{225}Ac-LMP1 tetramers effectively killed the targeted LMP1 CD8+ T-cell clones at small doses *in vitro* (ED_{50} = 5 – 8 nCi/mL or 0.001–0.0016 mg/mL). In contrast, the armed ^{225}Ac-LMP1 tetramers at 5 to 8 nCi/mL, exhibited much less toxicity to control Flu-specific CD8+ T cells. Nonspecific cytotoxicity could be induced at 15- to 40-fold-higher doses (ED_{50} = 110–200 nCi) when using [^{225}Ac]DOTA alone as a control. Much greater amounts of unlabeled, specific LMP1 tetramers (0.100–0.140 mg/mL) were needed to induce mild cytotoxicity in the targeted CD8+ T cells.

In a murine system, specific and potent cell killing by ^{225}Ac-LLO91-99 tetramers was also demonstrated. LLO91-99 peptide–specific CD8+ T cells were effectively killed after incubation with ^{225}Ac-LLO91-99 tetramers. The specificity in this T-cell killing using

the ^{225}Ac-LLO91-99 tetramers was demonstrated by blocking with the addition of a 50-fold excess of unlabeled LLO91-99-specific tetramers.

A demonstration that the cell killing by ^{225}Ac-LLO91-99 tetramers of LLO91-99 peptide–specific CD8+ T cells was selective was undertaken using a mixture of possible target cells. ^{225}Ac-LLO91-99 tetramers at concentrations of 1 to 30 nCi/mL (0.0002–0.006 mg/mL) were added to mixed cultures of LLO91-99-specific CD8+ and p60217–225-specific CD8+ T cells. After a 72-hour incubation with ^{225}Ac-LLO91-99 tetramers, significant cell killing was demonstrated in the whole population as judged by [^{3}H]thymidine incorporation and confirmed by reductions in viable cells determined with trypan blue staining. When the remaining viable cells in the population were analyzed by tetramer flow cytometry to define their specificities, there was a significant reduction in LLO91-99-specific CD8+ T cells ($P < 0.001$). In contrast, the nontargeted p60217-225-specific CD8+ T-cell population in the mixed cell culture showed only modest reductions even when exposed to higher quantities of ^{225}Ac-LLO91-99 tetramer (10 nCi/mL or 0.002 mg/mL).

These results demonstrate that ^{225}Ac-labeled tetramers can selectively delete both numbers and function of specific cytotoxic T lymphocytes (CTLs) with high specificity and induce little cytotoxicity within the other CD8+ T-cell populations.

4.3.2 Targeting small molecules—Small molecules as carriers for isotopes have been proposed for other alpha emitters like the 45 min half-life ^{213}Bi and the 7.2 h half life ^{211}At for targeting somatostatin receptor expression tumors [47, 48]. However, one main property of small molecules hampers their application: after application a relative high distribution volume is reached quickly. This occurs in a similar time in that the radioactive decay of these nuclides occurs. Thus, rapid excretion of small molecules will not be advantageous when used with short lived isotopes. In contrast, ^{225}Ac might be an interesting candidate for small molecules when high tumor retention can be achieved. Rapid excretion of small-molecule-^{225}Ac constructs will then diminish its toxicity significantly.

In preliminary experiments toxicity of [^{225}Ac]DOTA-Biotin and [^{225}Ac]DOTATOC was determined clinically and by weight measurements in BALB/c mice. [^{225}Ac]DOTA-Biotin can be utilized for several pretargeting approaches and [^{225}Ac]DOTATOC might be usable for somatostatin receptor radionuclide therapy. In both studies weight loss was observed in a fraction of animals but lethal toxicity was not observed until 60 kBq [^{225}Ac]DOTATOC at 180 days (n = 5) and until 740 kBq [^{225}Ac]DOTA-Biotin at 110 days (n = 3). Weight loss was predominant in the first 20 days and for animals injected with [^{225}Ac]DOTA-Biotin, weight recovery was remarkably better than for animals injected with [^{225}Ac]DOTATOC. (Miederer, et al. unpublished).

As preclinical evidence supports repeated dosing schedules, the rapid excretion of small molecules might display an advantage especially when repeated dosing schedules are used.

4.3.3 Novel carbon nanotube constructs—Devices constructed from novel nanotechnological platforms are envisioned that will incorporate features designed to target, bind, report, and irradiate tumor in vivo. Drugs have been investigated which inhibit tumor growth or are cytotoxic to tumor, however, despite the rapid accessibility of these agents to a variety of different molecular receptors expressed on tumor, many of the current targeting molecules suffer from low potency and specificity, weak binding interaction, rapid clearance, and a limited number of target molecules. We hypothesize that novel synthetic nanostructures based on molecules consisting of biologics, radionuclides and carbon nanotubes will have emergent anti-cancer properties and the stoichiometric amplification of the intrinsic targeting, binding, and therapeutic attributes of this nanodevice should therefore

improve potency, specificity, and efficacy relative to conventional anti-angiogenic agents. Such structures, containing multiple copies of covalently attached antibodies, chelated radiometals, and fluorochromes independently appended to a soluble carbon nanotube scaffold have been shown to target lymphoma in vitro and in vivo in a murine model [49]. Prototypes of these targeting nanoconstruct were applied to mice (doses of 0.5 mg/kg) and imaged [50]. The constructs rapidly clear the blood ($t_{1/2}$ < 1 h) and have some accumulation in liver, spleen and kidney. They are excreted in the urine. More work is necessary to develop and evaluate this technology.

5 Pharmacokinetic control of the parent and daughter radionuclides

5.1 Domain deleted Antibody fragments

It was hypothesized that if one were arming an antibody with ^{225}Ac and it did not form an internalizing antibody-antigen complex, then a smaller domain-deleted fragment of that antibody could better extravasate and penetrate the tumor where the decay daughters would remain localized as compared to the native, full-sized IgG [51]. The monoclonal antibody CC49 and the humanized domain-deleted product, ΔCH_2CC49, were converted to metal-binding constructs by appending the HEHA chelate, radiolabeled with ^{225}Ac, and evaluated for biodistribution, microdistribution, and therapeutic efficacy in ICR-SCID and nu/nu mouse models with s.c. and/or i.m. LS174T xenografts.

The %ID/g of [^{225}Ac]HEHA-CC49, [^{225}Ac]HEHA-ΔCH_2CC49, and [225Ac]HEHA-labeled control antibody that accumulated in the s.c. tumors after 24 h was 24.5, 18.2, and 10.1 and 8.1, 9.2, and 4.9 in the i.m. tumors, respectively. Liver and spleen accumulated ^{225}Ac which increased over days 1–8, presumably due to leakage out of the HEHA chelate. The retention of the daughters was investigated by calculating the ratio of ^{213}Bi to ^{225}Ac in the tumors over an 8 day period and it was found that there was little difference between the CC49 and the domain-deleted fragment. Autoradiographic analysis of tumor microdistribution demonstrated little difference in the antibodies. In both cases, the radionuclide was deposited close to the blood vessels in the tumor.

In the initial therapy study, 800 nCi of [^{225}Ac]HEHA-CC49, [^{225}Ac]HEHA- ΔCH_2CC49, or [225Ac]HEHA-control were administered to the ICR-SCID/LS174T (n = 10 per group) animal models having both s.c. and i.m. xenografts, nine days post-tumor implant. The MTD of the ^{225}Ac-construct was 800 nCi in these animals and all animals exhibited signs of radiotoxicity by day 6 and were sacrificed on day 8. There was no statistical difference in the tumor sizes in this study based upon treatment regimen. A second study was conducted in a NIH Swiss nu/nu/LS174T (n = 9–10 per group) animal models, nine days post tumor implant. Animals had either a s.c. or i.m. implant but not both. Animals with i.m. tumors responded best to treatment with 500 nCi [^{225}Ac]HEHA-CC49, with statistically smaller tumors than those treated with [^{225}Ac]HEHA-ΔCH_2CC49, control [225Ac]HEHA-IgG, or cold, unlabeled CC49. Animals with s.c. tumors all responded to treatment with 500 nCi [^{225}Ac]HEHA-CC49, [^{225}Ac]HEHA-ΔCH_2CC49, or control [225Ac]HEHA-IgG, but the latter two groups suffered from radiotoxicity. A third therapy study focused on the NIH Swiss nu/nu/LS174T (n = 10 per group) animal model, treated 6 days post tumor implant and treated with 0, 250, or 500 nCi of [^{225}Ac]HEHA-ΔCH_2CC49 or 500 nCi of the [225Ac]HEHA-IgG control. Animals had either a s.c. or i.m. implant but not both. There were no statistical differences in the tumor sizes per group in the s.c. implant groups. It was concluded that only marginal therapeutic effect could be attained with the [^{225}Ac]HEHA-CC49 and no therapeutic effect was observed using the domain-deleted fragment. The therapy was limited by radiotoxicity to normal organs.

5.2 Liposomal carriers

Novel liposomal carriers were designed and constructed to enhance the retention of the α-particle emitting daughters of ^{225}Ac in targeting applications as a way to control the pharmacokinetics of the daughters and utilize their cytotoxic potential [52]. Confinement of α-particle emitting daughters at the target sites increases efficacy while escape and redistribution throughout the body increases toxicity. Liposomal encapsulation of ^{225}Ac demonstrated that daughter retention was liposome-size dependent, but was lower than expected, due to binding of ^{225}Ac to the phospholipid membrane. To increase daughter retention, ^{225}Ac was passively entrapped in multivesicular liposomes (MUVEL). MUVELs are large liposomes with entrapped smaller lipid-vesicles, containing ^{225}Ac. This strategy provides confinement of entrapped ^{225}Ac within the region of the liposomal core, away from the outer liposomal membrane. PEGylated MUVELs yielded 98% ^{225}Ac retention, and 18% retention of the last daughter ^{213}Bi for 30 days. MUVELs were then conjugated to an anti-HER2/neu antibody, trastuzumab, and exhibited strong binding to and significant internalization (83%) by ovarian carcinoma SKOV3 cells. The i.p. administration of ^{225}Ac-containing MUVELs to animals with disseminated i.p. tumors, significant tumor uptake of ^{225}Ac and its daughters was detected.

^{228}Ac was employed as a substitute for ^{225}Ac and ^{223}Ra to investigate the encapsulation of nanogenerator nuclides in liposomes. Incorporation of 61 ± 8% (n = 3) was reported with ^{228}Ac by the ionophore loading method at 65°C for 30 min. The retention of ^{228}Ac in liposomes that were incubated in human serum was 95 ± 2% (n = 3) after 24 hours [53].

5.3 Cleavable linkages between the chelate moiety and the targeting molecule

Another strategy to alter the pharmacokinetics of the parent radionuclide entailed allowing sufficient time for the radioimmunoconstruct to target and then effect cleavage between the chelating moiety and the carrier molecule [54, 55]. This strategy was employed with DOTA chelated ^{225}Ac and used cleavable peptide linkages to append the chelated ^{225}Ac to the targeting antibody by Antczak *et al.* [56]. This study examined a construct that contained a bifunctional linker that was sensitive to cathepsins and compared that construct with a non-cleavable construct in vitro and in vivo. Specific release of ^{225}Ac from the carrier IgG was demonstrated by incubation with purified cathepsin B in vitro. However in HL60 tumor cells, mouse serum and mouse liver, the degradation of the cleavable and the non-cleavable linkers was similar. Biodistribution studies in mice showed a 2–3 fold higher liver uptake of ^{225}Ac when used with the cleavable linker. The authors attributed this to the fact that the maleimide linkage used might affect the biodistribution of the carrier construct.

5.4 Pharmacological interventions

The combined effects of stable chelation of ^{225}Ac for *in vivo* applications, efficient targeting of cell specific antigens and epitopes, and the internalization of the targeted constructs led to a potent and effective therapeutic nanogenerator strategy with no acute systemic toxicity. In particular, the internalization of the ^{225}Ac-labeled construct coupled with the stable DOTA chelation has proved useful in harnessing the cytotoxic potential of the daughters and mitigating their effects if redistributed. However, further efforts to understand the pharmacokinetics of the errant progeny of ^{225}Ac and the elucidation of ways to control their distribution have been described in order to have a better idea of the consequences in vivo [57].

[^{225}Ac]DOTA-IgG was prepared as described [27] and 500 nCi was administered i.v. to groups of mice. Metal chelation with 2,3-dimercapto-1-propanesulfonic acid (DMPS) or meso-2,3-dimercaptosuccinic acid (DMSA) caused a significant reduction ($p < 0.0001$) in the renal ^{213}Bi uptake; however, DMPS was more effective than DMSA ($p < 0.001$). Figure

4 contains biodistribution data at 24 hours for [^{225}Ac]DOTA-HuM195 administered to two cynomolgus monkeys. Note the reduction in the renal ^{213}Bi activity in the DMPS-treated monkey as compared to an untreated (no DMPS) animal. In mice, the renal ^{213}Bi and ^{221}Fr activities were significantly reduced by diuresis with furosemide or chlorothiazide (CTZ) treatment ($p < 0.0001$). The effect on renal ^{213}Bi activity was further enhanced by the combination of DMPS with either CTZ or furosemide ($p < 0.0001$). Competitive antagonism by bismuth subnitrate (BSN) moderately reduced the renal uptake of ^{213}Bi. The presence of a target-tumor sink significantly prevented the renal ^{213}Bi accumulation ($p = 0.003$), which was further reduced by DMPS treatment ($p < 0.0001$). The results indicate that metal chelation, diuresis with furosemide or CTZ, and competitive metal blockade may be considered as adjuvant therapies to modify the potential nephrotoxicity of ^{225}Ac daughters. Furthermore, delivery and internalization of the parent construct to a tumor site also decreased non-specific organ uptake of ^{213}Bi. These strategies may permit dose escalation of ^{225}Ac in a clinical setting.

The cyclotron production of ^{132}Cs from a natural xenon gas target was undertaken in order to study the pharmacokinetics of an individual short-lived daughter nuclide, ^{221}Fr [58]. The choice of cesium as an analogue for francium was predicated upon both elements being Group 1A alkali metals (cesium and francium have [Xe]$6s^1$ and [Rn]$7s^1$ electronic configurations, respectively) and cesium radionuclide possessed a longer half-life ($t_{1/2}$ = 6.48 days) to allow complete biodistribution studies to be performed. In order to determine whether ^{132}Cs was biochemically analogous to ^{221}Fr, a source of ^{221}Fr had to be developed for comparison. An ^{225}Ac /^{221}Fr generator was designed and its construction executed. Briefly, a DOTA-biotin construct [46] was labeled with ^{225}Ac and then was reacted with an immobilized avidin column. The generator was assayed in a dose calibrator at secular equilibrium. The generator was eluted with 2 mL of normal sterile saline yielding predominantly ^{221}Fr activity. The gamma energy spectrum was determined at 2 minutes and the ratio of ^{221}Fr/^{213}Bi was 13.5 (not decay corrected). This elution procedure yields predominantly ^{221}Fr (90%) with a small ^{213}Bi (10%) component at the time of detection. The counting window used to analyze the tissue activity was set to measure the ^{221}Fr photo peak (218 keV) only with little or no contribution from Compton Scatter from the higher energy ^{213}Bi photo peak (440 keV). In the ^{221}Fr biodistribution only blood and kidneys were harvested and counted because of the short nuclide half-life. For these studies the generator was eluted on average every 20 minutes yielding approximately 0.048 mCi of ^{221}Fr of which 0.006 mCi was injected per mouse. The %ID/g of ^{221}Fr was 52.3 ± 8.4 and 5.4 ± 0.3 in the kidneys and blood of these animals ($n = 3$), respectively. Cs-132 was provided by the MSKCC Cyclotron Core Facility. The %ID/g of ^{132}Cs was 33.0 ± 7.7 and 0.48 ± 0.05 in the kidneys and blood of these animals ($n = 3$), respectively. This data suggests that ^{132}Cs is not biochemically analogous to ^{221}Fr in mice. Both these radionuclides have 1 valence electron in the s-orbital, however, francium has a complete 4f and 5d shell of electrons. Since there is very little known about the chemistry of francium, we wanted to explore the correlation of its biodistribution properties *in vivo* with those of ^{132}Cs to see if there was analogous behavior. Since there was no correlation, one must conclude that the complete 4f and 5d shell of electrons in francium significantly change this ions chemistry relative to cesium.

6 Radiobiology

6.1 Consequences of non-specific internal radiation from the daughters

Some of the daughter radionuclides that were released systemically accumulated in the kidneys. The renal tubulointerstital changes that follow internal irradiation with alpha-particle emitting ^{225}Ac daughters was described in order to elucidate the radiobiological effects of the daughters in the kidney [59]. The histopathological evaluation of two

cynomolgus monkeys which received in a dose escalation schedule of three increasing [^{225}Ac]DOTA-HuM195 doses a cumulative activity of 377 kBq/kg, revealed mainly renal tubular damage associated with interstitial fibrosis [41]. The mechanism of radiation nephropathy resulting from targeted radionuclide therapies is poorly understood.

Naive Balb/c mice were administered 350 nCi of [^{225}Ac]DOTA-HuM195. The resulting functional and morphological changes in mice kidneys after injection with the construct were assessed chronologically. Renal irradiation from free, radioactive daughters of ^{225}Ac, led to time-dependant reduction in renal function manifesting as pallor and an increase in blood urea nitrogen. Corresponding histopathological changes were observed in the kidneys. Glomerular and tubular cell nuclear pleomorphism, karyorrhexis, tubular cell injury and lysis were observed as early as 10 weeks. Progressive thinning of the cortex due to widespread tubulolysis, collapsed tubules, glomerular crowding, decrease in glomerular cellularity and interstitial inflammation and an elevated juxtaglomerular index were noted at 20 – 30 weeks post treatment. By 35 – 40 weeks, regeneration of simplified tubules with tubular atrophy and loss and focal interstitial fibrosis had occurred. A lower juxtaglomerular cell index with focal cytoplasmic vacuolization, suggesting increased degranulation, was also observed in this period. Increased tubular and interstitial TGF-$\beta_1$expression and a corresponding increase in the extracellular matrix deposition was noticed only at 40 weeks post injection. These findings suggest that internally delivered alpha particle radiation-induced loss of tubular epithelial cells triggers a chain of adaptive changes that result in progressive morphological damage accompanied by a loss of renal function.

6.2 Pharmacological interventions

The radiation nephropathy following internal alpha particle irradiation of kidneys was ameliorated by pharmacologically modifying the functional and morphological changes in mouse kidneys following injection of 350 nCi of [^{225}Ac]DOTA-HuM195 using different agents [60]. This amount of activity delivers a dose of 27.6 Gy to the kidneys. Mice were randomized to receive captopril (ACE inhibitor), L-158,809 (Angiotensin II receptor-1 blocker), spironolactone (aldosterone receptor antagonist) or a placebo control. Forty weeks after [^{225}Ac]DOTA-HuM195 injection, placebo-control mice showed significant increase in BUN (87.6 ± 6.9 mg/dl), dilated Bowman spaces and tubulolysis with basement membrane thickening. Captopril treatment accentuated the functional (BUN = 119.0 ± 4.0 mg/dL; $p < 0.01$ vs. placebo controls) and histopathological damage. The Angiotensin II receptor-1 blocker, L-158,809 offered moderate protection (BUN = 66.6 ± 3.9 mg/dL; $p = 0.02$ vs. placebo controls). Spironolactone treatment, however, significantly prevented the development of histopathological and functional changes (BUN = 31.2 ± 2.5 mg/dL; $p < 0.001$ vs. placebo controls). In conclusion, low-dose spironolactone, and to a lesser extent, angiotensin receptor-1 blockade, offered renal protection in a mouse model of internal alpha particle irradiation.

7 Dosimetry

A schema was developed for estimating absorbed dose to organs following the administration of radionuclides with multiple unstable daughters in order to model the dosimetry of ^{225}Ac its daughters [61]. The dosimetry of alpha particle emitters requires that all decays, including those of unstable intermediates be included in the calculation. These calculations were further complicated by the potential differential biologic distribution of each of the progeny due to their different periodic properties. A formalism was presented which accounted for the known biodistribution factors of the daughters and the resulting effective biodistribution which depended upon the site at which the parent radionuclide decays. The number of decays or cumulated activity of a daughter radionuclide present in a particular tissue was estimated using a probability matrix which described the likelihood of

daughter decay in a particular tissue as a function of the decay site of the parent. Provided was an example of three initial compartments to illustrate the use of this formalism.

Cellular dose conversion factors (DCF) for α-particle-emitting radionuclides of interest in radionuclide therapy were calculated whereby the dose contribution of daughter radionuclides at the site of parent decay was made dependent on a cut-off time parameter, which was used to estimate the fraction of daughter decays expected at the site of parent decay [62]. Previously tabulated S values (cell-surface to nucleus and cell-surface to cell) for each daughter were scaled by this fraction. Then a sum over all daughters was performed to yield a cut-off time-dependent set of corresponding DCF values for each radionuclide. These DCF values for the absorbed dose to the nuclear or cellular volume arising from cell-surface decays were presented as a function of the cut-off time for 4 different representative sets of cellular and nuclear dimensions. In contrast to the cellular S values that account only for the parent nuclide decay, these cellular dose conversion factors values made it possible to easily include the contribution of daughter decays in cellular alpha-particle emitter dose calculations.

The theoretical estimation of absorbed dose to key organs using radionuclides with multiple unstable daughters was made using three different models [63]. Since each of the progeny of ^{225}Ac has its own free-state biodistribution and characteristic half-life, then their inclusion for a more accurate prediction of absorbed dose and potential toxicity requires a formalism that takes these factors into consideration. Model 1 restricted the transport to a function that yielded either the place of origin or the place(s) of biodistribution depending on the half-life of the parent radionuclide. Model 2 included the transient time in the bloodstream and model 3 incorporated additional binding at or within the tumor. This means that model 2 also allows for radionuclide decay and further daughter production while moving from one location to the next and that model 3 relaxes the constraint that the residence time within the tumor is solely based on the half-life of the parent. Simulated were both a 0.1 g rapidly accessible tumor and a 10 g solid tumor. Additionally, the effects of varying radiolabled carrier molecule purity and mass amount of carrier molecules, as well as tumor cell antigen saturation were examined. The results indicated that there was a distinct advantage in using a parent radionuclide such as ^{225}Ac, having a half-life of 10 days and yielding 4 alpha particles per decay, because lower doses to normal organs resulted for a given tumor dose in comparison to those radionuclides yielding fewer alpha particles.

Dosimetry calculations where applied to the study of [^{225}Ac]DOTA-HuM195 in cynomolgus monkeys [41]. The measured time activity curves for ^{225}Ac and for ^{213}Bi in blood where used to estimate blood and renal cortex doses. All ^{213}Bi disintegrations not occurring in blood where assigned to the renal cortices. The assumption was made that the location of the ^{221}Fr and ^{217}At daughter nuclide's decays were based upon the site of the ^{225}Ac decay (blood or renal cortex). These estimations - assuming a homogenous energy deposition of the alpha radiation - resulted in renal cortex doses ranging from 3 Gy (^{221}Fr and ^{217}At decay at site of ^{225}Ac decay) to 13 Gy (^{221}Fr and ^{217}At decay at site of ^{225}Ac decay) for a cumulated dose of 1.89 MBq [^{225}Ac]DOTA-HuM195 (377 kBq/kg).

8 Clinical trials

Recently, the first patients were treated with [^{225}Ac]DOTA-HuM195 in a Phase I clinical trial at Memorial Sloan-Kettering Cancer Center. At press, the seventh patient had been treated at a third dose level, receiving 0.173 mCi of ^{225}Ac (0.002 mCi/kg) on 1.7 mg HuM195 (0.020 mg/kg). Patient accrual continues.

This phase I clinical trial with [^{225}Ac]DOTA-HuM195 resulted from a period of clinical investigation of CD33-targeted therapy in patients with AML, mainly relapsed or refractory.

Early studies were conducted with the murine form, M195, labeled with ^{131}I in patients with minimal residual disease (50 to 70 mCi/m^2) or to intensify therapy prior to bone marrow transplant (BMT) (120–230 mCi/m^2). However, the detection of human anti-mouse antibodies in a fraction of patients precludes additional M195 treatments in the further course of the disease [64]. The humanized form of this antibody, HuM195, demonstrated a lack of immunogenicity and an increased affinity to CD33. Intensification of therapy prior to BMT might be achieved with the longer ranged beta-emitter yttrium-90 and further clinical studies where conducted with ^{90}Y labeled HuM195 for myeloablation [65]. In contrast, in non-myeloablative regimens, CD33 negative stem cells have to be spared from the non-specific cross radiation. This led to the strategy that employed the alpha-emitting nuclide Bismuth-213 labeled to HuM195. In a Phase I clinical trial, the anti-leukemic effect of [^{213}Bi]-HuM195 was demonstrated in patients with relatively high tumor burden [17]. Because of the large tumor burden in AML, the Phase I/II study used a regimen wherein Cytarabine was given prior to the [^{213}Bi]-HuM195 to effect some cytoreduction before alpha-particle therapy. This led to the first clinical trial using the longer-lived and more potent ^{225}Ac in humans using the [^{225}Ac]DOTA-HuM195 construct [18].

9 References Cited

1. Milenic DE, Brechbiel MW. Targeting of radio-isotopes for cancer therapy. Cancer Biology & Therapy. 2004; 3:361–370. [PubMed: 14976424]
2. Nikula TK, McDevitt MR, Finn RD, Wu C, Kozak RW, Garmestani K, Brechbiel MW, Curcio MJ, Pippin CG, Tiffany-Jones L, Geerlings MW Sr, Apostolidis C, Molinet R, Geerlings MW Jr, Gansow OA, Scheinberg DA. Alpha-emitting bismuth cyclohexylbenzyl DTPA constructs of recombinant humanized anti-CD33 antibodies: pharmacokinetics, bioactivity, toxicity and chemistry. J Nucl Med. 1999; 40:166–176. [PubMed: 9935073]
3. Couturier O, Supiot S, Degraef-Mougin M, Faivre-Chauvet A, Carlier T, Chatal JF, Davodeau F, Cherel M. Cancer radioimmunotherapy with alpha-emitting nuclides. European Journal of Nuclear Medicine and Molecular Imaging. 2005; 32:601–614. [PubMed: 15841373]
4. Friesen C, Glatting G, Koop B, Schwarz K, Morgenstern A, Apostolidis C, Debatin KM, Reske SN. Breaking chemoresistance and radioresistance with [213Bi]anti-CD45 antibodies in leukemia cells. Cancer Research. 2007; 67:1950–1958. [PubMed: 17332322]
5. McDevitt MR, Ma D, Lai LT, Simon J, Borchardt P, Frank RK, Wu K, Pellegrini V, Curcio MJ, Miederer M, Bander NH, Scheinberg DA. Tumor therapy with targeted atomic nanogenerators. Science. 2001; 294:1537–1540. [PubMed: 11711678]
6. McDevitt MR, Barendswaard E, Ma D, Lai L, Curcio MJ, Sgouros G, Ballangrud AM, Yang WH, Finn RD, Pellegrini V, Geerlings MW Jr, Lee M, Brechbiel MW, Bander NH, Cordon-Cardo C, Scheinberg DA. An alpha-particle emitting antibody ([213Bi]J591) for radioimmunotherapy of prostate cancer. Cancer Research. 2000; 60:6095–6100. [PubMed: 11085533]
7. Weast, RC. 66th Edition of the CRC Handbook of Chemistry and Physics. CRC Press, Inc; Boca Raton, FL: 1985.
8. Adloff JP. The centenary of a controversial discovery: actinium. Radiochim Acta. 2000:123–127.
9. Methods for the production of Ac-225 and Bi-213 for alpha immunotherapy, ITU Annual Report 1995-(EUR 16368)-Basic Actinide Research 1995, pp. 55–56.
10. Koch, L.; Apostolidis, C.; Molinet, R.; Nicolaou, G.; Janssens, W.; Schweikert, H. Production of Bi-213 and Ac-225, Alpha-Immuno-97 Symposium; Karlsruhe, Germany. 1997.
11. Mirzadeh S. Generator-produced alpha-emitters. Appl Radiat Isot. 1998; 49:345–349.
12. Apostolidis C, Molinet R, Rasmussen G, Morgenstern A. Production of Ac-225 from Th-229 for targeted alpha therapy. Analytical chemistry. 2005; 77:6288–6291. [PubMed: 16194090]
13. Boll RA, Malkemus D, Mirzadeh S. Production of actinium-225 for alpha particle mediated radioimmunotherapy. Appl Radiat Isot. 2005; 62:667–679. [PubMed: 15763472]
14. Boll RA, Mirzadeh S, Kennel SJ, DePaoli DW, Webb OF. Bi-213 for alpha particle mediated radioimmunotherapy. J Label Compds and Radiopharm. 1997; 40:341–343.

15. McDevitt MR, Finn RD, Ma D, Larson SM, Scheinberg DA. Preparation of alpha-emitting 213Bi-labeled antibody constructs for clinical use. J Nucl Med. 1999; 40:1722–1727. [PubMed: 10520715]
16. McDevitt MR, Finn RD, Sgouros G, Ma D, Scheinberg DA. An 225Ac/213Bi generator system for therapeutic clinical applications: construction and operation. Appl Radiat Isot. 1999; 50:895–904. [PubMed: 10214708]
17. Jurcic JG, Larson SM, Sgouros G, McDevitt MR, Finn RD, Divgi CR, Ballangrud AM, Hamacher KA, Ma D, Humm JL, Brechbiel MW, Molinet R, Scheinberg DA. Targeted alpha particle immunotherapy for myeloid leukemia. Blood. 2002; 100:1233–1239. [PubMed: 12149203]
18. Jurcic JG, McDevitt MR, Pandit-Taskar N, Divgi CR, Finn RD, Sgouros G, Apostolidis C, Chanel S, Larson SM, Scheinberg DA. Alpha-particle immunotherapy for acute myeloid leukemia (AML) with Bismuth-213 and Actinium-225. Cancer Biotherapy and Radiopharmaceuticals. 2006; 21(4): 396.
19. Geerlings MW, Kaspersen FM, Apostolidis C, van der Hout R. The feasibility of 225Ac as a source of alpha-particles in radioimmunotherapy. Nuclear Medicine Communications. 1993; 14:121–125. [PubMed: 8429990]
20. Khalkin VA, Tsoupka-Sitnikoz VV, Zaitseva NG. Radionuclides for radiotherapy. Properties, preparation and application of Actinium-225. Radiochemistry. 1997; 39:483–492.
21. Lambrecht RM, Tomiyoshi K, Sekine T. Radionuclide Generators. Radiochimica Acta. 1997; 77:103–123.
22. Apostolidis C, Molinet R, McGinley J, Abbas K, Mollenbeck J, Morgenstern A. Cyclotron production of Ac-225 for targeted alpha therapy. Appl Radiat Isot. 2005; 62:383–387. [PubMed: 15607913]
23. McDevitt MR, Sgouros G, Finn RD, Humm JL, Jurcic JG, Larson SM, Scheinberg DA. Radioimmunotherapy with alpha-emitting nuclides. European Journal of Nuclear Medicine. 1998; 25:1341–1351. [PubMed: 9724387]
24. Diamond R, Street K, Seaborg GT. An ion-exchange study of possible hybridized 5f bonding in the actinides. J Am Chem Soc. 1954; 76:1461–1469.
25. Yamana H, Mitsugashira T, Shiokawa Y, Sato A, Suzuki S. Possibility of the existence of divalent actinium in aqueous solution. J Radioanalytical Chem. 1983; 76:19–26.
26. Kulikov EV, Novgorodov AF, Schumann D. Hydrolysis of ^{225}Actinium trace quantities. J Radioanal Nucl Chem, Letters. 1992; 164:103–108.
27. McDevitt MR, Ma D, Simon J, Frank RK, Scheinberg DA. Design and synthesis of 225Ac radioimmunopharmaceuticals. Appl Radiat Isot. 2002; 57:841–847. [PubMed: 12406626]
28. Taylor DM. The metabolism of actinium in the rat. Health Physics. 1970; 19:411–418. [PubMed: 5512923]
29. Barr, GC. USAECReport. UCRL; 1955. Tracer studies with actinium-227; p. 5-10.
30. Campbell JE, Robajdek ES, Anthony DS. The metabolism of Ac-227 and its daughters Th-227 and Ra-223 by rats. Radiation Research. 1956; 4:294–302. [PubMed: 13310749]
31. Jolley RD, Horne WPR, Anthony DS. The effects of injected actinium equilibrium on rats and mice. Mound Laboratory Report MLM-1057. 1955:1–8.
32. Newton D. A case of accidental inhalation of protactinium-231 and actinium-227. Health Physics. 1968; 15:11–17. [PubMed: 5743753]
33. Beyer GJ, Bergmann R, Schomacker K, Rosch F, Schafer G. Comparison of the biodistribution of ^{225}Ac and radio-lanthanides as citrate complexes. Isopenpraxis. 1990; 3:111–114.
34. Beyer GJ, Offord R, Kunzi G, Aleksandrova Y, Ravn U, Jahn S, Barker J, Tengblad O, Lindroos M. The influence of EDTMP-concentration on the biodistribution of radio-lanthanides and 225-Ac in tumor-bearing mice. The ISOLDE Collaboration. Nuclear Medicine and Biology. 1997; 24:367–372. [PubMed: 9290069]
35. Davis IA, Glowienka KA, Boll RA, Deal KA, Brechbiel MW, Stabin M, Bochsler PN, Mirzadeh S, Kennel SJ. Comparison of 225actinium chelates: tissue distribution and radiotoxicity. Nuclear Medicine and Biology. 1999; 26:581–589. [PubMed: 10473198]

36. Deal KA, Davis IA, Mirzadeh S, Kennel SJ, Brechbiel MW. Improved in vivo stability of actinium-225 macrocyclic complexes. Journal of Medicinal Chemistry. 1999; 42:2988–2992. [PubMed: 10425108]
37. Kaspersen FM, Bos E, Doornmalen AV, Geerlings MW, Apostolidis C, Molinet R. Cytotoxicity of 213Bi- and 225Ac-immunoconjugates. Nuclear Medicine Communications. 1995; 16:468–476. [PubMed: 7675360]
38. Chappell LL, Deal KA, Dadachova E, Brechbiel MW. Synthesis, conjugation, and radiolabeling of a novel bifunctional chelating agent for (225)Ac radioimmunotherapy applications. Bioconjugate Chemistry. 2000; 11:510–519. [PubMed: 10898572]
39. Kennel SJ, Chappell LL, Dadachova K, Brechbiel MW, Lankford TK, Davis IA, Stabin M, Mirzadeh S. Evaluation of 225Ac for vascular targeted radioimmunotherapy of lung tumors. Cancer Biotherapy & Radiopharmaceuticals. 2000; 15:235–244. [PubMed: 10941530]
40. Borchardt PE, Yuan RR, Miederer M, McDevitt MR, Scheinberg DA. Targeted actinium-225 in vivo generators for therapy of ovarian cancer. Cancer Research. 2003; 63:5084–5090. [PubMed: 12941838]
41. Miederer M, McDevitt MR, Sgouros G, Kramer K, Cheung NK, Scheinberg DA. Pharmacokinetics, dosimetry, and toxicity of the targetable atomic generator, 225Ac-HuM195, in nonhuman primates. J Nucl Med. 2004; 45:129–137. [PubMed: 14734685]
42. Miederer M, McDevitt MR, Borchardt P, Bergman I, Kramer K, Cheung NK, Scheinberg DA. Treatment of neuroblastoma meningeal carcinomatosis with intrathecal application of alpha-emitting atomic nanogenerators targeting disialo-ganglioside GD2. Clin Cancer Res. 2004; 10:6985–6992. [PubMed: 15501978]
43. Ballangrud AM, Yang WH, Palm S, Enmon R, Borchardt PE, Pellegrini VA, McDevitt MR, Scheinberg DA, Sgouros G. Alpha-particle emitting atomic generator (Actinium-225)-labeled trastuzumab (herceptin) targeting of breast cancer spheroids: efficacy versus HER2/neu expression. Clin Cancer Res. 2004; 10:4489–4497. [PubMed: 15240541]
44. Nolan DJ, Ciarrocchi A, Mellick AS, Jaggi JS, Bambino K, Gupta S, Heikamp E, McDevitt MR, Scheinberg DA, Benezra R, Mittal V. Bone marrow-derived endothelial progenitor cells are a major determinant of nascent tumor neovascularization. Genes & Development. 2007; 21:1546–1558. [PubMed: 17575055]
45. Singh Jaggi J, Henke E, Seshan SV, Kappel BJ, Chattopadhyay D, May C, McDevitt MR, Nolan D, Mittal V, Benezra R, Scheinberg DA. Selective alpha-particle mediated depletion of tumor vasculature with vascular normalization. PLoS ONE. 2007; 2:e267. [PubMed: 17342201]
46. Yuan RR, Wong P, McDevitt MR, Doubrovina E, Leiner I, Bornmann W, O'Reilly R, Pamer EG, Scheinberg DA. Targeted deletion of T-cell clones using alpha-emitting suicide MHC tetramers. Blood. 2004; 104:2397–2402. [PubMed: 15217835]
47. Norenberg JP, Krenning BJ, Konings IR, Kusewitt DF, Nayak TK, Anderson TL, de Jong M, Garmestani K, Brechbiel MW, Kvols LK. 213Bi-[DOTA0, Tyr3]octreotide peptide receptor radionuclide therapy of pancreatic tumors in a preclinical animal model. Clin Cancer Res. 2006; 12:897–903. [PubMed: 16467104]
48. Vaidyanathan G, Boskovitz A, Shankar S, Zalutsky MR. Radioiodine and 211At-labeled guanidinomethyl halobenzoyl octreotate conjugates: potential peptide radiotherapeutics for somatostatin receptor-positive cancers. Peptides. 2004; 25:2087–2097. [PubMed: 15572196]
49. McDevitt MR, Chattopadhyay D, Kappel BJ, Jaggi JS, Schiffman SR, Antczak C, Njardarson JT, Brentjens R, Scheinberg DA. Tumor targeting with antibody-functionalized, radiolabeled carbon nanotubes. J Nucl Med. 2007; 48:1180–1189. [PubMed: 17607040]
50. McDevitt MR, Chattopadhyay D, Jaggi JS, Finn RD, Zanzonico PB, Njardarson JT, Scheinberg DA. Positron-Emission Tomographic (PET) Imaging of Soluble Carbon Nanotubes in Mice. PLoS ONE. 2007; 2:e907. [PubMed: 17878942]
51. Kennel SJ, Brechbiel MW, Milenic DE, Schlom J, Mirzadeh S. Actinium-225 conjugates of MAb CC49 and humanized delta CH2CC49. Cancer Biotherapy & Radiopharmaceuticals. 2002; 17:219–231. [PubMed: 12030116]

52. Sofou S, Kappel BJ, Jaggi JS, McDevitt MR, Scheinberg DA, Sgouros G. Enhanced Retention of the Alpha-particle Emitting Daughters of Actinium-225 by Liposome Carriers. Bioconjugate Chemistry. 2007 in press.

53. Henriksen G, Schoultz BW, Michaelsen TE, Bruland OS, Larsen RH. Sterically stabilized liposomes as a carrier for alpha-emitting radium and actinium radionuclides. Nuclear Medicine and Biology. 2004; 31:441–449. [PubMed: 15093814]

54. Kukis DL, Novak-Hofer I, DeNardo SJ. Cleavable linkers to enhance selectivity of antibody-targeted therapy of cancer. Cancer Biotherapy & Radiopharmaceuticals. 2001; 16:457–467. [PubMed: 11789023]

55. Quadri SM, Vriesendorp HM. Effects of linker chemistry on the pharmacokinetics of radioimmunoconjugates. J Nucl Med. 1998; 42:250–261.

56. Antczak C, Jaggi JS, LeFave CV, Curcio MJ, McDevitt MR, Scheinberg DA. Influence of the linker on the biodistribution and catabolism of actinium-225 self-immolative tumor-targeted isotope generators. Bioconjugate Chemistry. 2006; 17:1551–1560. [PubMed: 17105236]

57. Jaggi JS, Kappel BJ, McDevitt MR, Sgouros G, Flombaum CD, Cabassa C, Scheinberg DA. Efforts to control the errant products of a targeted in vivo generator. Cancer Research. 2005; 65:4888–4895. [PubMed: 15930310]

58. Finn R, McDevitt MR, Sheh Y, Lom C, Qiao J, Cai S, Burnazi E, Nacca A, Pillarsetty N, Jaggi J, Scheinberg DA. Cyclotron Production of Cesium Radionuclides as Analogues for Francium-221 Biodistribution. Nucl Instrum Methods. 2005; 241:649–651.

59. Jaggi JS, Seshan SV, McDevitt MR, LaPerle K, Sgouros G, Scheinberg DA. Renal tubulointerstitial changes after internal irradiation with alpha-particle-emitting actinium daughters. J Am Soc Nephrol. 2005; 16:2677–2689. [PubMed: 15987754]

60. Jaggi JS, Seshan SV, McDevitt MR, Sgouros G, Hyjek E, Scheinberg DA. Mitigation of radiation nephropathy after internal alpha-particle irradiation of kidneys. International Journal of Radiation Oncology, Biology, Physics. 2006; 64:1503–1512.

61. Hamacher KA, Sgouros G. A schema for estimating absorbed dose to organs following the administration of radionuclides with multiple unstable daughters: a matrix approach. Medical Physics. 1999; 26:2526–2528. [PubMed: 10619234]

62. Hamacher KA, Den RB, Den EI, Sgouros G. Cellular dose conversion factors for alpha-particle--emitting radionuclides of interest in radionuclide therapy. J Nucl Med. 2001; 42:1216–1221. [PubMed: 11483682]

63. Hamacher KA, Sgouros G. Theoretical estimation of absorbed dose to organs in radioimmunotherapy using radionuclides with multiple unstable daughters. Medical Physics. 2001; 28:1857–1874. [PubMed: 11585217]

64. Jurcic JG, Caron PC, Nikula TK, Papadopoulos EB, Finn RD, Gansow OA, Miller WH Jr, Geerlings MW, Warrell RP Jr, Larson SM, et al. Radiolabeled anti-CD33 monoclonal antibody M195 for myeloid leukemias. Cancer Research. 1995; 55:5908s–5910s. [PubMed: 7493368]

65. Jurcic JG, Divgi CR, McDevitt MR, Ma D, Sgouros G, Finn RD, Larson SM, Scheinberg DA. Potential for myeloablation with yttrium-90 labeled HuM195 (anti-CD33): a Phase I trial in advanced myeloid leukemias. Blood. 1998; 92(10):613A.

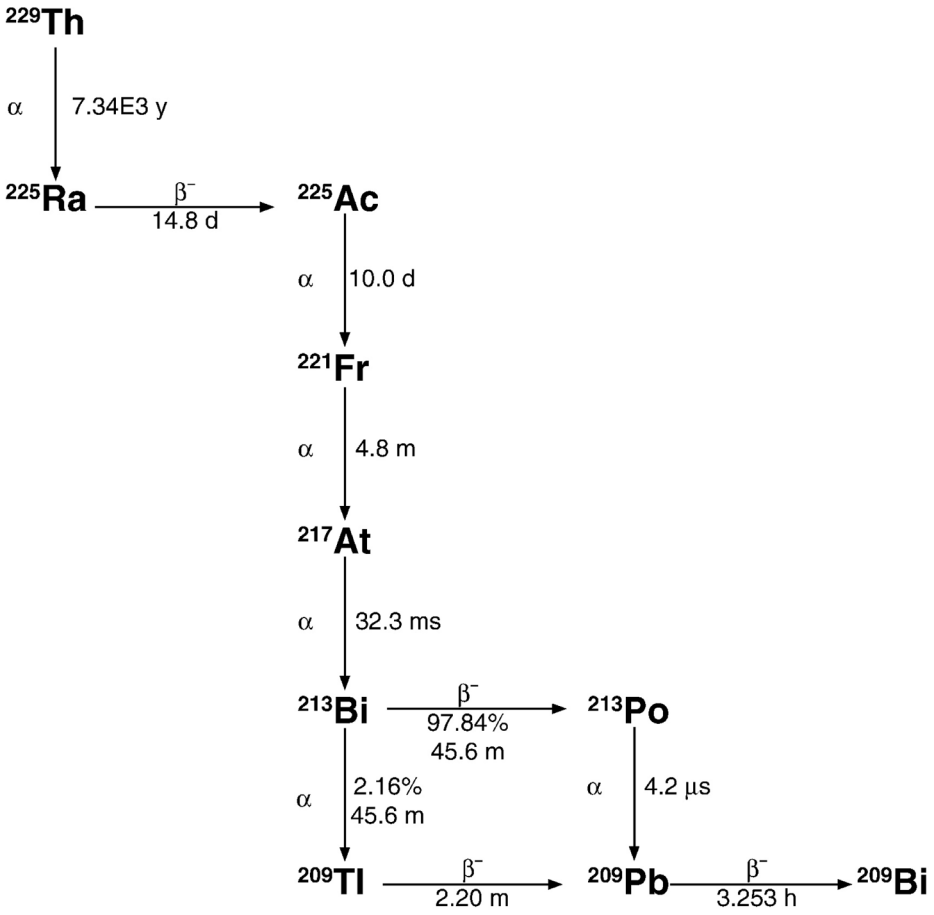

Figure 1.
The ^{229}Th decay scheme.

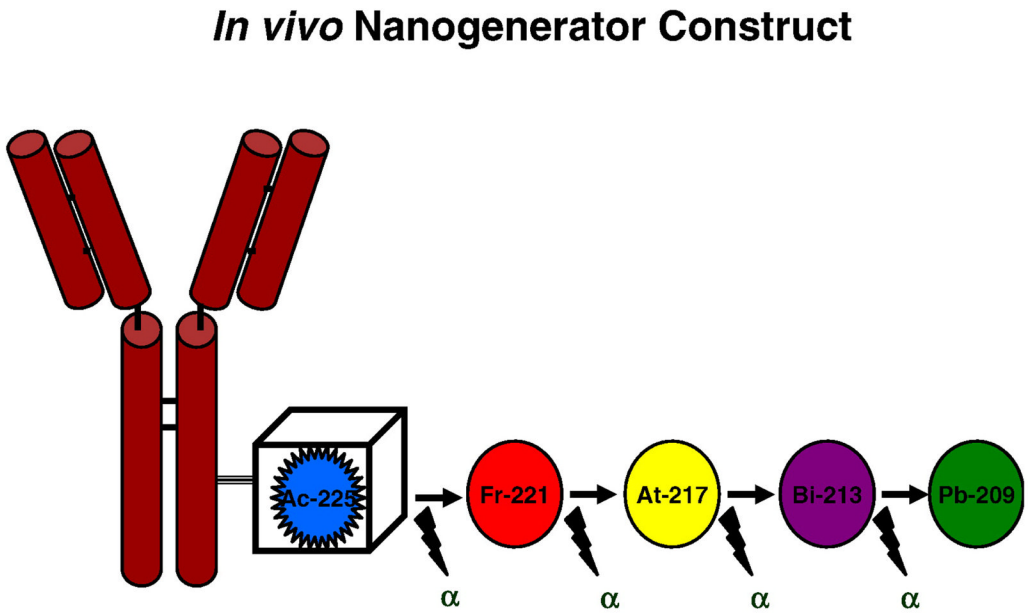

Figure 2.
An illustration of the ^{225}Ac nanogenerator system.

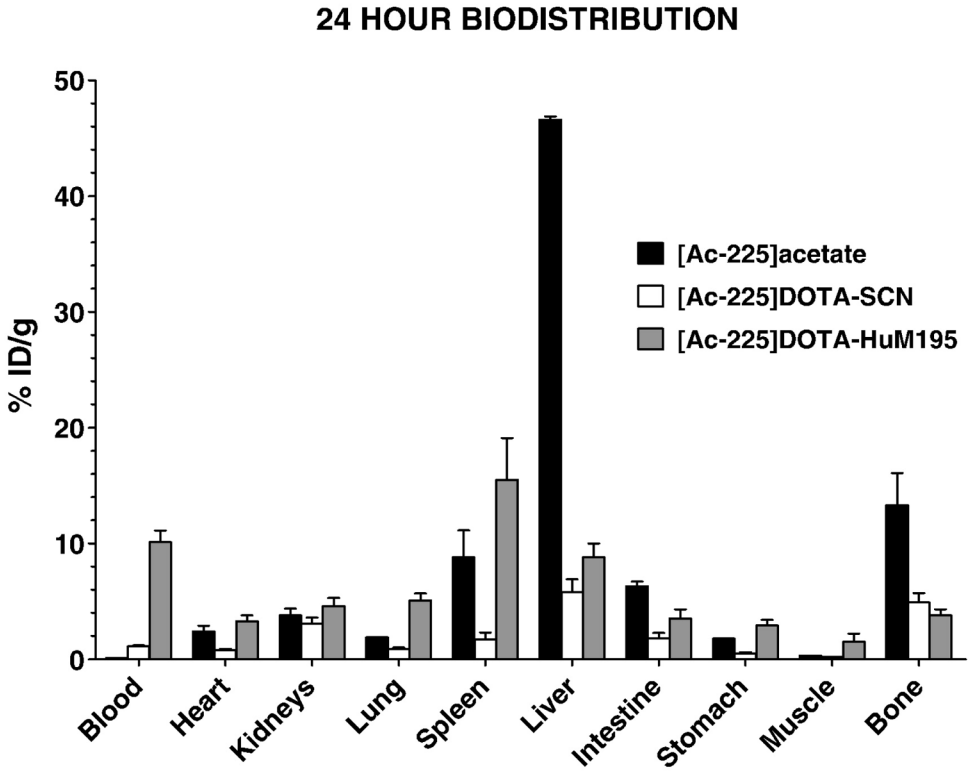

Figure 3.
Murine biodistribution data at 24 hours for ^{225}Ac-acetate, [^{225}Ac]DOTA-SCN, and [^{225}Ac]DOTA-HuM195.

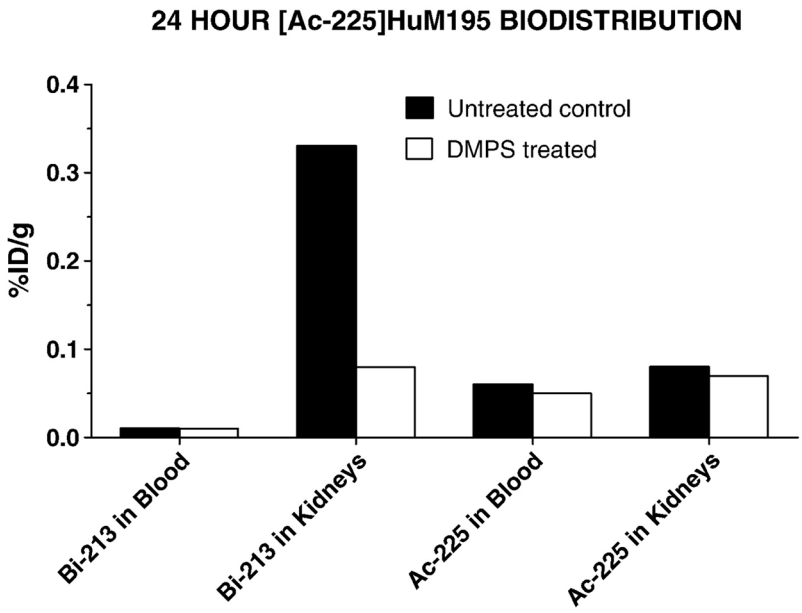

Figure 4.

Biodistribution data at 24 hours for [^{225}Ac]DOTA-HuM195 administered to two cynomolgus monkeys. Note the reduction in the renal ^{213}Bi activity in the DMPS-treated monkey as compared to an untreated (no DMPS) animal.